JOURNAL OF MATERIALS SCIENCE 24 (1989) 510–514

# Rate sensitivity in the high temperature deformation of dispersion strengthened Al–Fe–V–Si alloys

G. S. MURTY
*Department of Metallurgical Engineering, Indian Institute of Technology, Kanpur, India*
M. J. KOCZAK
*Department of Materials Engineering, Drexel University, Philadelphia, Pennsylvania 19104, USA*

The rate sensitive flow characteristics in the elevated temperature deformation of Al–Fe–V–Si alloys processed by rapid solidification/powder metallurgy route were assessed by the strain rate change tests in compression. With an ultrafine grain size, stabilized by fine dispersoids, a peak rate sensitivity index of ~0.15 and normal ductility were observed in alloys containing dispersoids up to a volume fraction of 0.37. The lack of superplastic response is interpreted in terms of a high threshold stress for superplastic flow. The threshold stress assessed by an extrapolation procedure is observed to be grain size and temperature dependent. Its origin is suggested to be Zener drag limited boundary migration, which is an essential part of the superplastic flow mechanism.

## 1. Introduction

A rapid solidification/powder metallurgy (PM) processing route results in significant improvements in properties through the refinement of dispersoid and grain sizes in structural aluminium alloys. This improvement in strength of PM wrought alloys is accompanied by a significant drop in their room temperature ductility and the formability at room temperature and elevated temperature may be limited. However, superplastic forming may be possible at elevated temperatures, because of their ultrafine grain size stabilized by dispersoids. Extended ductility and high strain rate sensitivity of flow stress were reported in such alloys at a relatively high strain rate range [1, 2]. The objective of this study was to assess the rate sensitivity of flow stress in the high temperature deformation of dispersion strengthened Al–Fe–V–Si alloys developed by Skinner *et al.* [3] and to interpret their rate sensitivity characteristics in terms of the mechanisms of elevated temperature deformation.

## 2. Experimental details

Three Al–Fe–V–Si alloys with different volume fraction of dispersoids processed at Allied Corporation, Morristown, New Jersey, were used for this study. Their compositions are listed in Table I and processing details are available in [3]. In brief, melt spun ribbons obtained from prealloyed compositions were comminuted into powders, vacuum hot pressed and extruded. A range of dispersoid volume fractions of 0.16, 0.26 and 0.37 was considered.

After annealing the extruded materials at 575° C for 100 h, right circular cylinder compression specimens of 6 mm diameter and 9 mm height were machined and tested at elevated temperatures. Strain rate change tests were performed on an Instron machine in compression at elevated temperatures using an elliptical radiant furnace. The true stress ($\sigma$)–true strain rate ($\dot{\varepsilon}$) data and the strain rate sensitivity index ($m = \text{dlog } \sigma / \text{dlog } \dot{\varepsilon}$) were computed from the load–compression data of the strain rate change tests.

The microstructures were characterized by transmission electron microscopy (TEM) with a JEM-100CX electron microscope. The thin foils for TEM were prepared by the jet polishing technique making use of an electrolyte of 1 : 3 nitric acid : methanol at − 30° C. The mean grain diameter assessed from the measurements of individual grains in electron micrographs is the reported grain size. The mean dispersoid size was determined by measuring particle sizes also from electron micrographs.

## 3. Results

### 3.1. Microstructural characterization

As a consequence of the processing route adopted in developing them, ultrafine equiaxed grains of ~0.5 $\mu$m size are stabilized by fine intermetallic particles of $Al_{12}(Fe, V)_3Si$ phase in these alloys [3]. The TEM

TABLE I Chemical compositions of the Al–Fe–V–Si alloys investigated

| Alloy number | Composition (wt %) | | | | Nominal volume fraction of dispersoids |
|---|---|---|---|---|---|
| | Fe | V | Si | Al | |
| 1 | 5.95 | 1.00 | 1.02 | Bal | 0.16 |
| 2 | 8.75 | 1.60 | 1.60 | Bal | 0.26 |
| 3 | 11.61 | 1.38 | 2.23 | Bal | 0.37 |


0022–2461/89 $03.00 + .12 

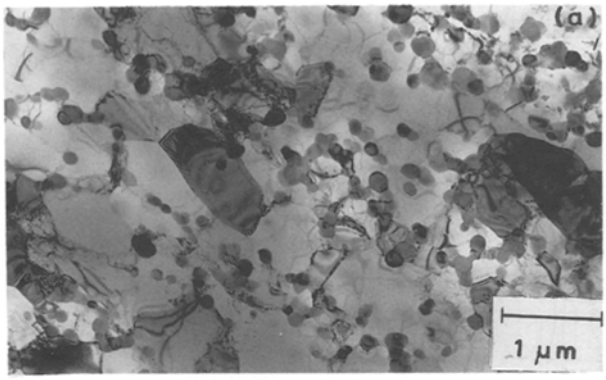


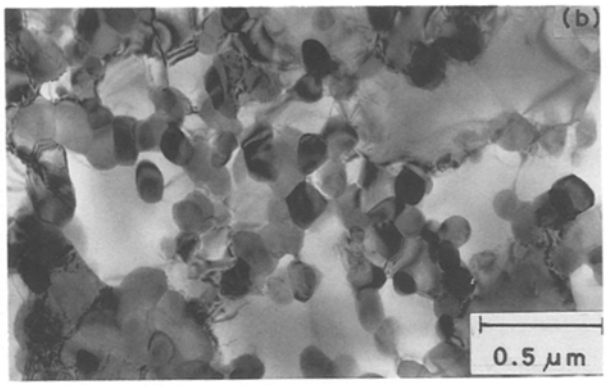


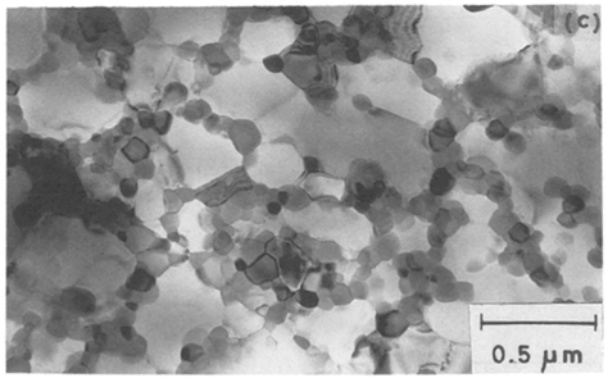


*Figure 1* TEM electron micrographs of (a) Alloy 1 ($V_f$ = 0.16) (b) Alloy 2 ($V_f$ = 0.27) and (c) Alloy 3 ($V_f$ = 0.37).

micrographs representing the microstructures of the three alloys are shown in Fig. 1. While the spread in the intermetallic particle size range is relatively narrow, the trend of clustering of the particles was noticed with the increase in the volume fraction of the second phase. The data pertaining to the grain size and particle size of the dispersed intermetallic phase are listed in Table II. Since the fine grain size is stabilized by the dispersoid pinning of grain boundaries, the grain size ($d$) can be estimated from the volume fraction ($V_f$) and particle radius ($r$) of the second phase making use of the Zener relation [4]

$$d = 4r/3V_f \quad (1)$$

While the grain size thus estimated compares favourably with the observation in alloy 1, there is an increasing degree of deviation in the other alloys, where the clustering of particles is prevalent.

### 3.2. Mechanical testing

The rate sensitivity of the flow behaviour of the alloys assessed by the strain rate change test at various temperatures is shown in Figs 2 to 4. Their strain rate sensitivity index ($m$) is relatively low, with a maximum of only $\sim 0.15$. Consequently, only normal ductility is expected and it is confirmed by tensile tests at elevated temperatures. The flow behaviour of the three alloys is compared in Fig. 5 for the highest test temperature of 575° C. While the nature of variation of "$m$" with strain rate is similar in all the alloys, the flow stress over the investigated strain rate range is seen to increase with the volume fraction of the intermetallic phase or the drop in grain size.

TABLE II Grain and particle sizes of the alloys

| Alloy number | Grain size ($\mu$m) | Particle diameter ($\mu$m) |
|---|---|---|
| 1 | 0.72 ± 0.239 | 0.15 ± 0.056 |
| 2 | 0.44 ± 0.089 | 0.14 ± 0.041 |
| 3 | 0.40 ± 0.092 | 0.08 ± 0.026 |

In order to assess the operative flow mechanisms, the steady state stress ($\sigma$)–strain rate ($\dot{\varepsilon}$) data were analysed by the empirical equation applicable to the elevated temperature deformation of fine grained materials

$$\dot{\varepsilon} = (AD_0Eb/kT)\,(b/d)^p\,(\sigma/E)^n \exp(-Q/RT) \quad (2)$$

where $A$ is a dimensionless constant, $D_0 \exp(-Q/RT)$ is the appropriate diffusion coefficient, $Q$ the activation energy, $E$ the modulus of elasticity, $\boldsymbol{b}$ Burgers vector, $T$ the absolute temperature, $d$ the grain size, $p$ the grain size exponent, $n(=1/m)$ the stress exponent, $k$ the Boltzmann constant and $R$ the gas constant. The activation energy for flow is determined from an Arrhenius plot of $\log(TE^{n-1}\sigma^{-n})$ at a constant strain rate against $1/T$. For this purpose, the variation of modulus of elasticity of aluminium with temperature as per the data in [5] was considered.

On the basis of the flow stress data corresponding to a constant $\dot{\varepsilon} = 2.4 \times 10^{-4}\,\text{sec}^{-1}$, the calculated values of activation energy for flow are 392 ± 46.4 (alloy 1), 447 ± 72.2 (alloy 2) and 490 ± 37.2 (alloy 3) kJ mol$^{-1}$. The corresponding Arrhenius plots are shown in Fig. 6. These activation energy values can be seen to be significantly higher than the activation energy for lattice self-diffusion in aluminium [5]. By assessing the grain size effect on flow stress at a given strain rate and test temperature, it is seen that the flow stress increases as the grain size decreases. These characteristics are similar to our recent observations in region I of superplastic Al–Zn–Mg–Cu–Mn [6] and Al–Ti [7] alloys.

## 4. Discussion

In view of the ultrafine grain size of these alloys, flow mechanisms applicable to superplasticity such as grain boundary sliding (GBS) and diffusional flow are expected to be operative during their high temperature deformation. Calculations based on theoretical constitutive relations for Nabarro–Herring [8] and Coble

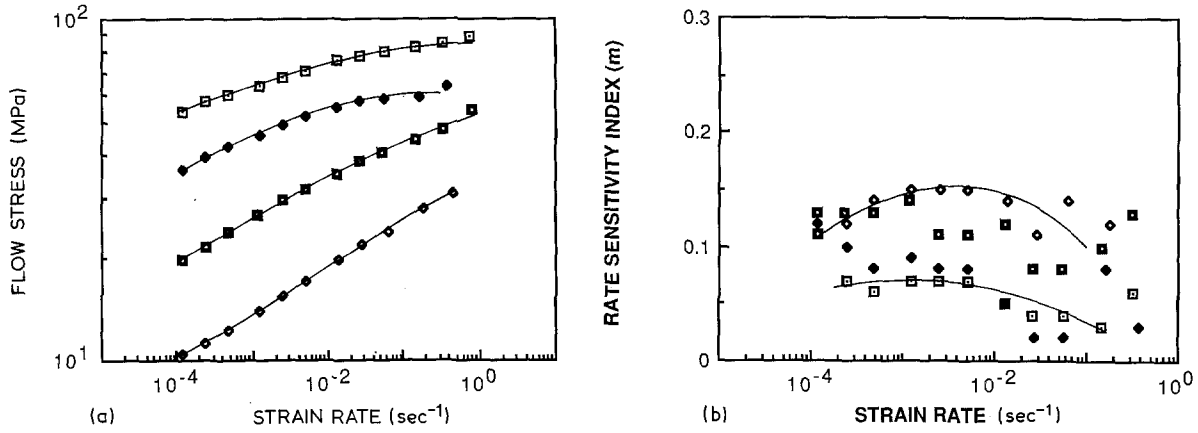


*Figure 2* Plots of (a) flow stress against strain rate and (b) strain rate sensitivity index ($m$) against strain rate for the alloy 1 ($V_f$ = 0.16) (□ 425° C, ◆ 475° C, ■ 525° C, ◇ 575° C).

creep [9] mechanisms indicate that the observed strain rates are two to three orders of magnitude lower than the predicted strain rates corresponding to the respective flow stresses of these alloys. Superplastic flow mechanisms such as the Ashby–Verrall model [10] predict even faster strain rates than the diffusional flow mechanisms. On the other hand, low rate sensitivity of flow stress and an increase in the rate sensitivity with strain rate at the lower end of the investigated strain rate range suggest their flow behaviour to be of the Bingham type. Moreover, an anomalously high activation energy for flow and the nature of grain size effect on flow stress which strongly resemble the region I characteristics of rapidly solidified powder aluminium alloys [6, 7] favour an interpretation in terms of a threshold stress for the superplastic flow mechanism.

Assuming that a threshold stress exists for the superplastic flow mechanism, which typically has an "$m$" value of 0.5, the threshold stress can be evaluated by an extrapolation of a double linear plot of $\sigma$ against $\dot{\varepsilon}^{0.5}$ at each test temperature. Such plots for the various alloys are shown in Fig. 7. Since the threshold stress, thus obtained is found to vary with temperature and grain size, the activation energy ($Q$) and the grain size exponent ($p$) for the threshold mechanism are evaluated making use of an empirical equation

$$\sigma_0/E = (K_1/d^p) \exp(Q/RT) \quad (3)$$

where $K_1$ is a constant. The Arrhenius plot based on Equation 3 is shown in Fig. 8 and the corresponding $Q$ values are 42.4 ± 7.8, 51 ± 7.6 and 55.1 ± 2.8 kJ $mol^{-1}$ for the alloys 1, 2 and 3 respectively. With reference to the evaluation of the grain size exponent, a linear regression fit of $p = 1$ is found to yield correlation coefficient in the range of 0.82 to 0.95 by considering the data at various test temperatures.

On the basis of the Ashby–Verrall model [10] of diffusionally accommodated grain boundary sliding (GBS) for superplastic flow, the threshold stress may arise from

(i) an increase in the grain boundary area during the grain neighbour switching events [10, 11]

(ii) the inability of the grain boundaries to act as perfect sinks and sources for point defects [12]

(iii) the inhibition of GBS by the dispersoids at the grain boundaries [13], and

(iv) the drag force on the boundaries due to Zener pinning by the dispersoids and thereby restricting the grain boundary migration (GBM) [6, 7].

While the Ashby–Verrall model [10] and its modification by Geckinli [11] predict a threshold stress on the basis of the increase in the grain boundary area during deformation, its magnitude or temperature dependence is too small relative to the present observations. If the grain boundaries are not perfect sinks and sources for point defects, the threshold stress can be identified with the stress needed to bow the grain boundary dislocations between the second phase particles [12]. However, the observed temperature dependence of

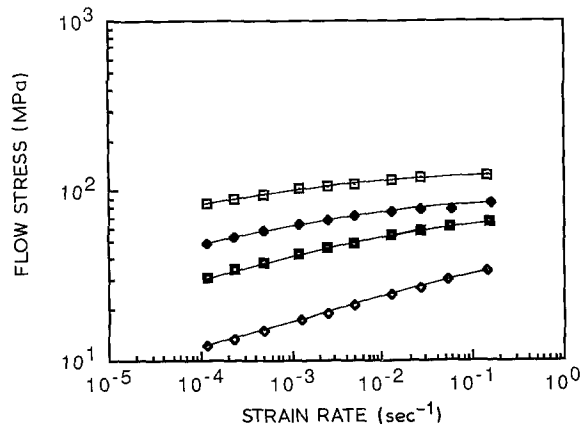


*Figure 3* Plot of flow stress against strain rate for the alloy 2 ($V_f$ = 0.26) (□ 425° C, ◆ 475° C, ■ 525° C, ◇ 575° C).

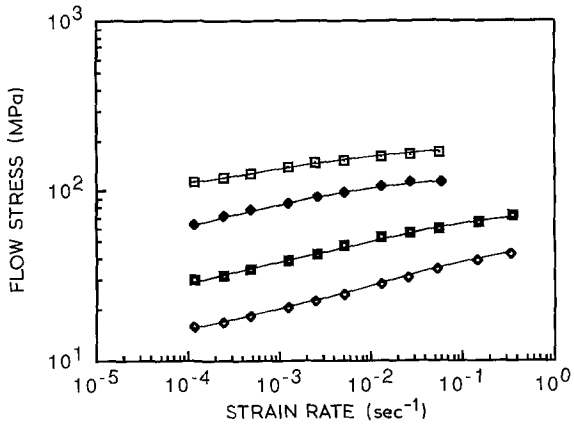


*Figure 4* As Fig. 3 for alloy 3 ($V_f$ = 0.37).

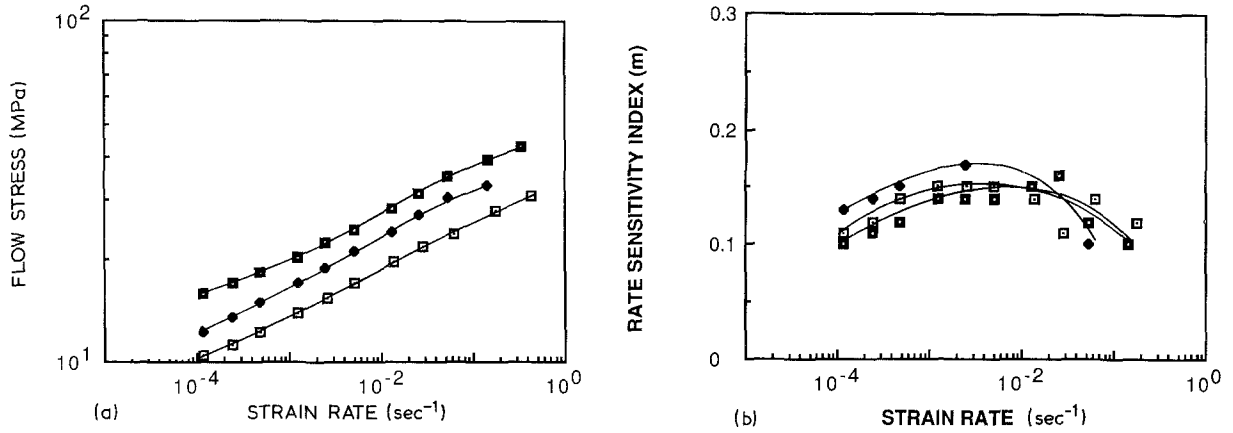


*Figure 5* A comparison of the plots of (a) flow stress against strain rate and (b) strain rate sensitivity index ($m$) against strain rate for the three alloys at the test temperature of 575° C. (□ $V_f$ = 0.16, ◆ $V_f$ = 0.26, ■ $V_f$ = 0.37).

the threshold stress cannot be predicted on this basis. Although the interaction between grain boundary dislocations and second phase particles or solute atoms predicts a threshold stress for GBS [13, 14], the observed effects of temperature and grain size on the threshold stress cannot be explained on this basis.

The drag effect of particles on boundary migration, i.e. process (iv), may possibly account for the observations relating to the threshold stress. GBM is an integral part of superplastic deformation, irrespective of the details of the flow mechanism as the grains remain equiaxed during superplastic deformation. In certain situations, GBM may become the rate controlling step during superplastic flow. When fine particles stabilize an ultrafine grain size, the drag force per unit area ($P$) on the boundary because of the pinning effect [4] is

$$P = 3V_f\gamma_b/2r \quad (4)$$

where $\gamma_b$ is the grain boundary energy. Combining Equations 1 and 4 we have

$$P = 2\gamma_b/d \quad (5)$$

Accordingly, the threshold stress arising from the Zener drag is expected to vary inversely with grain size. Since the mobility of grain boundaries is a thermally activated process, the threshold stress arising from the restricted mobilities of the grain boundaries may be temperature dependent with an activation energy characteristic of the grain boundary migration process. Considering the activation energy obtained from the temperature dependence of the threshold stress observed in this study, it is seen that it is in agreement with that for boundary migration in aluminium [15, 16]. Although the observed grain size and temperature effects of the threshold stress can thus be interpreted in terms of the Zener drag mechanism, the

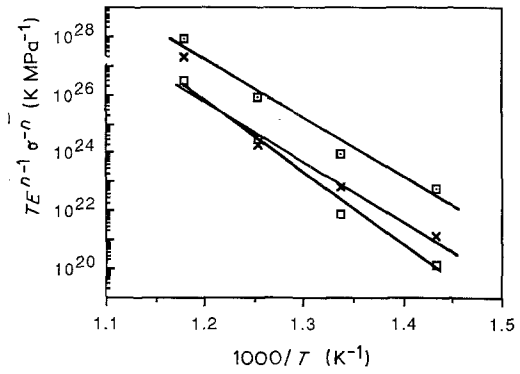


*Figure 6* Arrhenius plot for the activation energy determination for flow (data correspond to a constant strain rate = 2.4 × $10^{-4}$ $sec^{-1}$). (⊡ alloy 1, x alloy 2, □ alloy 3) for Al–Fe–V–Si alloys.

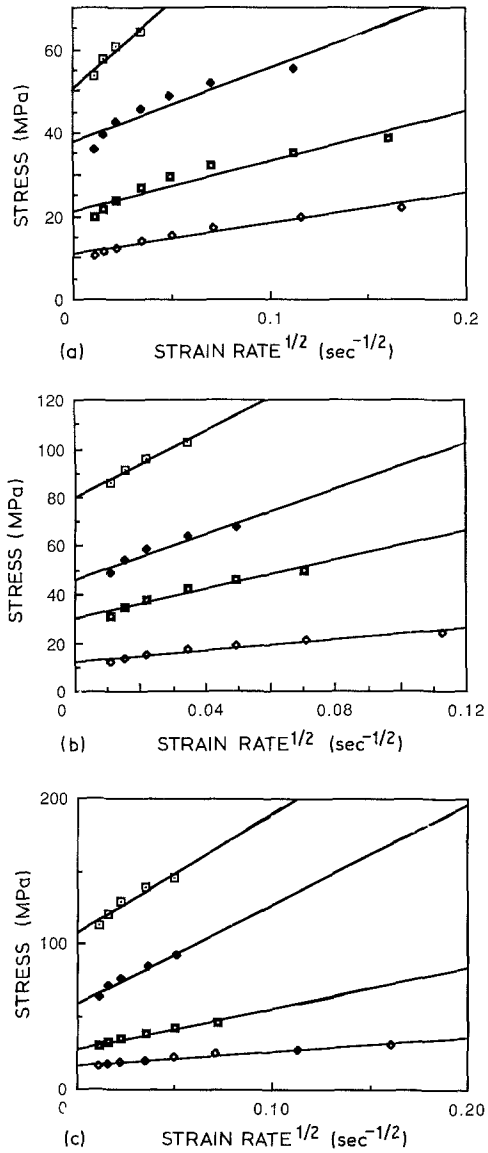


*Figure 7* Determination of the threshold stress through extrapolation for (a) Alloy 1 (b) Alloy 2 and (c) Alloy 3. (□) 425° C, ◆ 475° C, ■ 525° C, ◇ 575° C).

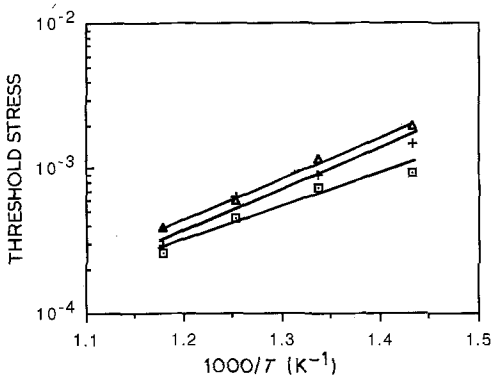


*Figure 8* Arrhenius plots for the determination of the activation energy for the threshold mechanism. (□ alloy 1, + alloy 2, △ alloy 3).

problem of quantitatively predicting the threshold stress on this basis remains to be considered.

Following the Bingham like behaviour of increasing rate sensitivity with strain rate in the lower strain rate range, the rate sensitivity index is observed to drop beyond a strain rate of $\sim 10^{-2}\,sec^{-1}$. This is a consequence of a change in mechanism towards an inherently low rate sensitive plastic flow mechanism of intragranular slip (region III). Thus the peak value of the rate sensitivity index attained in the superplastic region II is dependent upon the magnitude of threshold stress for superplastic flow on the one hand and the onset of region III on the other.

## 5. Conclusions

(1) The maximum strain rate sensitivity index attained at elevated temperatures in these dispersion strengthened alloys is $\sim 0.15$ despite their ultrafine grain size.

(2) The elevated temperature flow stress in the investigated strain rate range is observed to increase with the volume fraction of the second phase, whereas it decreases with the grain size.

(3) On the basis of (i) the increase in the rate sensitivity index with strain rate (Bingham flow) at the lower strain rate range (ii) an anomalously high activation energy for flow and (iii) the grain size effect on flow stress, the lack of superplastic response of these ultrafine grained alloys is interpreted in terms of a threshold stress for superplastic flow.

(4) Making use of an extrapolation procedure, the threshold stress was estimated and it is found to be grain size and temperature dependent. The origin of the threshold stress for superplastic flow is suggested to be the restricted mobility of grain boundaries because of Zener drag.

## Acknowledgements

We thank Dr D. J. Skinner of Allied Corporation, Morristown, New Jersey for providing the alloys for this study. This work was supported by the Naval Air Development Center, Warminster, Pennsylvania.

## References

1. T. G. NIEH and J. WADSWORTH, in "Superplasticity in Aerospace Aluminum", edited by R. Pearce and L. Kelly (Cranfield, UK, 1986) p. 194.
2. G. S. MURTY and M. J. KOCZAK, in "Powder Metallurgy Composites", edited by P. Kumar, K. Vedula and A. Ritter (The Metallurgical Society, 1988) p. 139.
3. D. J. SKINNER, R. L. BYE, D. RAYBOULD and A. M. BROWN, *Scripta Metall.* **20** (1986) 867.
4. C. S. SMITH, *Trans. Met. Soc. AIME* **175** (1948) 15.
5. L. F. MONDOLFO, "Aluminum Alloys: Structure and Properties", (Butterworths, London, 1979) p. 82.
6. G. S. MURTY and M. J. KOCZAK, *Mater. Sci. Eng.* **96** (1987) 117.
7. *Idem, ibid.*, in press.
8. C. HERRING, *J. Appl. Phys.* **21** (1950) 437.
9. R. L. COBLE, *ibid.* **34** (1963) 1679.
10. M. F. ASHBY and R. A. VERRALL, *Acta Metall.* **21** (1973) 149.
11. A. E. GECKINLI, *Metal Sci.* **17** (1983) 12.
12. E. ARZT, M. F. ASHBY and R. A. VERRALL, *Acta Metall.* **31** (1983) 1977.
13. M. F. ASHBY, *Surface Sci.* **31** (1972) 498.
14. C. A. P. HORTON, *Scripta Metall.* **8** (1974) 1.
15. C. FROIS and O. DIMITROV, *Ann. Chim.* **1** (1966) 113.
16. R. FROMAGEAU, *Mem. Sci. Rev. Metall.* **LXVI** (1969) 287.

*Received 19 January*
*and accepted 1 June 1988*